International Journal of Pharmaceutics 400 (2010) 158–164

Contents lists available at ScienceDirect

International Journal of Pharmaceutics

journal homepage: www.elsevier.com/locate/ijpharm

Pharmaceutical Nanotechnology

Third generation solid dispersions of ferulic acid in electrospun composite nanofibers

Deng-Guang Yu[a], Jian-Mao Yang[b], Christopher Branford-White[c], Ping Lu[b], Li Zhang[b], Li-Min Zhu[a,*]

[a] College of Chemistry, Chemical Engineering and Biotechnology, Donghua University, Shanghai 201620, China
[b] Center of Analysis & Measurement, Donghua University, Shanghai 201620, China
[c] Institute for Health Research and Policy, London Metropolitan University, London N7 8DB, UK

ARTICLE INFO

Article history:
Received 29 June 2010
Received in revised form 2 August 2010
Accepted 6 August 2010
Available online 14 August 2010

Keywords:
Solid dispersions
Composite nanofibers
Electrospinning
Ferulic acid

ABSTRACT

Third generation solid dispersions (SDs) of ferulic acid (FA) in composite nanofibers were prepared using electrospinning. The spinning liquids involved co-dissolving solutions of FA, polyvinylpyrrolidone (PVP), sodium dodecyl sulfate (SDS) and sucralose in 75% ethanol aqueous solutions. FESEM observations showed that the nanofibers were assembled in a homogeneous web structure that had a smooth cross-section and surface with an average diameter of 254 ± 32 nm. Results from DSC and XRD suggested that FA, SDS and sucralose were distributed in the PVP fibers in an amorphous manner and this is due to their compatibility resulting through a second-order interactions, as demonstrated by ATR-FTIR spectra. *In vitro* dissolution and permeation tests showed that the nanofiber-based SDs could release all the contained FA within 1 min and had a 13-fold higher permeation rate across sublingual mucosa compared to crude FA particles. The casting films have the same compositions as the nanofibers and belong to the third generation SDs, they gave the same solubility of FA as the nanofibers, and also exhibited a much faster dissolution rate than pure FA particles. It felt that electrospinning can be taken to prepare new generation SDs with structural characteristics that enhancing absorbance of poorly soluble drugs.

1. Introduction

Currently about 40% or more of drugs in development and about 60% of molecules obtained directly from synthesis are directly obtained from the synthesis of poorly soluble molecules in aqueous media. The solubility behavior of poorly water-soluble drugs remains one of the most challenging aspects of the formulation development in pharmaceutics. Many processes and technologies have been tried in order to provide more effective and versatile approaches to address formulation issues (Vasconcelos et al., 2007; Leuner and Dressman, 2000).

Solid dispersion (SD) is one of the more promising strategies to improve the oral bioavailability of poor water-soluble drugs. It refers to a group of solid products consisting of at least two different components, generally consisting of a hydrophilic matrix and a hydrophobic drug. SDs are usually presented as amorphous products that are mainly obtained by two different methods, for example, melting and solvent evaporation (Chokshi et al., 2007; Dhirendra et al., 2009).

Researches about new SDs and the related fabrication processes have been widely reported in literature during the past several decades, and now a few SD products have been marketed (Vasconcelos et al., 2007). Recently, it has been shown that the dissolution profile can be improved if the carrier has surface activity or self-emulsifying properties, therefore developing a third generation SDs appeared. They often consist of the active pharmaceutical ingredient (API), an amorphous polymers and surfactants. The third generation SD is intended to achieve a higher degree of bioavailability for poorly soluble drugs to stabilize the SD, avoiding drug re-crystallization. The processes for developing the third generation SDs often adopt traditional evaporation methods. New and optimized manufacturing processes for producing third generation SDs are desired (Vasconcelos et al., 2007).

Electrospinning, derived from "electrostatic spinning", has regained more attention and this is probably due in part to a surging interest in nanotechnology, as ultrafine fibers or fibrous structures of various polymers with diameters in the submicron/nanometer range can be easily fabricated (Formhals, 1934; Doshi and Reneker, 1995; Dzenis, 2004). The electrospinning process is very similar to the solvent evaporation methods for preparing SD, as far as the removing of solvent is concerned. During the electrospinning process, when the polymer jet is ejected and accelerated toward the collector solvent evaporation is rapid (often in milliseconds) as the high surface area jet travels towards the target. As an outcome,

* Corresponding author at: College of Chemistry, Chemical Engineering and Biotechnology, Donghua University, 2999 North Renmin Road, Songjiang District, Shanghai 201620, China. Tel.: +86 21 67792748; fax: +86 21 62372655.
E-mail address: lzhu@dhu.edu.cn (L.-M. Zhu).

0378-5173/$ – see front matter © 2010 Elsevier B.V. All rights reserved.
doi:10.1016/j.ijpharm.2010.08.010

the non-woven filament mats are quickly formed and this leads to a decrease in drug mobility. When solvent evaporation is complete, drug molecules are often 'frozen' in the polymer fibers matrix (Burke and Luzhansky, 2007; Yu et al., 2009a,b, 2010a). Based on the possibly favored interactions between the drug and polymer, a crystal lattice is not created, and the drug molecules are randomly 'ordered' in the fiber matrix. Therefore amorphous SDs with the random distribution of APIs may be produced through a simple and straightforward one-step process.

A number of laboratories have shown that double components SDs in electrospun nanofibers could improve the dissolution rates of poorly water-soluble drugs. In this system itraconazole and ibuprofen were used as model drugs, and hydroxypropylmethylcellulose (HPMC) and polyvinylpyrrolidone (PVP) as filament-forming matrix and drug carriers, respectively (Verreck et al., 2003; Yu et al., 2009a). Recently Yu and coworkers also compared SDs of acetaminophen/PVP using different processes and the results demonstrated that electrospun nanofiber-based SDs showed better enhanced dissolution effects compared to other casting-film SDs prepared using traditional processes such as vacuum drying, freeze drying, and heat-drying (Yu et al., 2010b).

However, all the fiber SDs mentioned above are two component systems. The addition of third or even the fourth functional components may provide the fiber SDs even greater performance. For example, the inclusion of surfactants in the formulation containing a polymeric carrier may both prevent precipitation and/or protect a fine crystalline precipitate from agglomeration into much larger hydrophobic particles (Vasconcelos et al., 2007). On the other hand, electrospinning is not only a simple straightforward process for fabricating nanofibers, but it also allows the co-processing of polymer mixtures or functional materials to provide a variety of pathways for controlling the chemical compositions of the prepared nanofibers and for tailoring them for specific functions (Huang et al., 2003; Li and Xia, 2004).

Ferulic acid (FA), 4-hydroxy-3-methoxycinnamic acid, is an antioxidant which neutralizes free radicals (superoxide, nitric oxide and hydroxyl radical) which could cause oxidative damage to cell membranes and DNA. FA may reduce the risk of many cancers, including cancer of the stomach, colon, breast, prostate, liver, lung and tongue. Studies also have shown that FA can decrease blood glucose levels and so could be applicable for the treatment of diabetes patients. However, the poor solubility of FA may impede its fast dissolution and absorption and thus result in poor bioavailability (Sohn and Oh, 2003; Kampa et al., 2004; Lee, 2005; Anselmi et al., 2008).

In this paper, using FA as the model drug, we describe the preparation and characterization of a novel type of third generation SDs in composite nanofibers. They were electrospun from co-dissolving solutions containing several functional ingredients. The aim is for synchronously improving dissolution rates and permeation profiles of the drug and providing a pleased taste for patients' convenience.

2. Experimental

2.1. Materials

FA was purchased from Shanghai Winherb Medical Sci & Tech Development Co., Ltd. (Shanghai, China). Polyvinylpyrrolidone K30 (PVP K30, M = 58,000 Da) was obtained from Shanghai Yunhong Pharmaceutical Aids and Technology Co., Ltd. (Shanghai, China). Sucralose, sodium dodecyl sulfate (SDS) and ethanol were provided by the Sinopharm Chemical Reagent Co., Ltd. All other chemicals used were analytical grade, and the water was highly purified water.

2.2. Preparation

2.2.1. Preparation of spinning solutions

The concentration of PVP K30 in the spinning solutions was fixed at 30% (w/v) according to pre-experiments about its filament-forming properties. The drug FA, PVP K30, the surfactant SDS and sucralose co-dissolved in 75% (v/v) ethanol aqueous solutions at the ambient temperature according to a weight ratio of 15:30:1:4. This gave a drug content of 30% in the solid fibers. Mechanical stirring was applied for at least 2 h to obtain homogeneous co-dissolved spinning solutions. The solutions were degassed with a SK5200H ultrasonator (350W, Shanghai Jinghong Instrument Co., Ltd., Shanghai, China) for 10 min before spinning.

2.2.2. Electrospinning process

A high voltage power supply (Shanghai Sute Electrical Co., Ltd.) was used to provide high voltages in the range of 0–60 kV. To avoid carrying any air bubbles, spinning solutions were carefully loaded in a 10 ml syringe to which a stainless steel capillary metal-hub needle was attached. The inside diameter of the metal needle was 0.5 mm. The positive electrode of the high voltage power supply was connected to the needle tip and the grounded electrode was linked to a metal collector wrapped with aluminum foil.

The electrospinning process was carried out under ambient conditions ($21 \pm 2\,^{\circ}C$ and relative humidity $57 \pm 3\%$). A fixed electrical potential of 12 kV was applied across a fixed distance of 15 cm between the tip and the collector. The feed rate of solutions was controlled at 3.0 ml h^{-1} by means of a single syringe pump (Cole-Parmer®, USA). The formed fibers were dried for over 24 h at 40 °C under vacuum (320 Pa) in a DZF-6050 Electric Vacuum Drying Oven (Shanghai Laboratory Instrument Work Co. Ltd., Shanghai, China). This facilitated the removal of residual organic solvent and moisture.

Casting films used as controls were prepared by maintaining the co-dissolving solutions at 70 °C for drying in an air-circulated oven until a constant weight was reached.

2.3. Characterization

2.3.1. Morphology

The morphology of the surface, cross-sections of the nanofiber mats and the casting films were assessed using a S-4800 field emission scanning electron microscope (FESEM) (Hitachi, Japan). The average fiber diameter was determined by measuring diameters of fibers at over 100 points from FESEM images using NIH Image J software (National Institutes of Health). Before carbon-coating, the cross-sections of the nanofiber mats were prepared by first placing them into liquid nitrogen and then they were broken manually.

2.3.2. DSC

The differential scanning calorimetry (DSC) analyses were carried out using an MDSC 2910 differential scanning calorimeter (TA Instruments Co., USA). Sealed samples were heated at 10 °C min^{-1} from 20 to 250 °C. The nitrogen gas flow rate was 40 ml min^{-1}.

2.3.3. XRD

X-ray diffraction analysis (XRD) were obtained on a D/Max-BR diffractometer (RigaKu, Japan) with Cu Kα radiation in the 2θ range of 5–60° at 40 mV and 300 mA.

2.3.4. ATR-FTIR

Attenuated total reflectance Fourier transform infrared (ATR-FTIR) analysis was carried out on a Nicolet-Nexus 670 FTIR spectrometer (Nicolet Instrument Corporation, Madison, USA) over the range 500–4000 cm^{-1} and a resolution of 2 cm^{-1}.

2.4. Solubility, in vitro dissolution and permeation tests

2.4.1. Solubility

An excess amount of FA crude particles, casting films and electrospun fibers was added to the aqueous solutions. The samples were allowed to shake for 48 h at 37 °C. 1 ml of the sample solution was drawn and filtered through a 0.22 μm (Millipore, USA) pore size filter and diluted using highly purified water to determine the FA content. All the measurements were carried out in triplicate.

2.4.2. In vitro dissolution tests

The *in vitro* dissolution tests were carried out according to the Chinese Pharmacopoeia (2005 ED.) Method II, a paddle method using a RCZ-8A dissolution apparatus (Tianjin University Radio Factory, China), was used. Composite nanofibers or casting films (330 mg), or 100 mg of crude FA particles (<100 μm) were put into 900 ml phosphate buffer (PBS, pH 6.8, 0.1 M) at 37 ± 1 °C and at 50 rpm, sink conditions $C < 0.2C_S$. At predetermined time intervals, samples of 5.0 ml were withdrawn and replaced with fresh medium to maintain constant volume. After filtration through a 0.22 μm membrane (Millipore, USA) and appropriate dilution with PBS, the sample solutions were analyzed at 322 nm by a UV spectrophotometer (Unico Instrument Co., Ltd., Shanghai, China). All the measurements were carried out in triplicate.

2.4.3. In vitro buccal permeation studies

The *in vitro* permeation studies were performed using a RYJ-6A Diffusion Test Apparatus (Shanghai Huanghai Drug Control Instrument Co., Ltd.), in which material were mounted in six Keshary–Chien glass diffusion cells and a water bath system that maintained a constant temperature, 37 ± 0.2 °C. Each cell had a diffusion area of 2.60 cm^2 and the receptor compartment had a capacity of 7.2 ml.

Porcine sublingual mucosae obtained from a local abattoir were mounted between the donor and receptor compartments of the diffusion cells with the mucosal surface uppermost. This occurred within 2 h of slaughtering. Each donor compartment was filled with 1 ml PBS and the hydrodynamics in the receptor compartment were maintained by stirring with a teflon coated magnetic bead at 100 rpm. The sublingual membranes were equilibrated for 30 min before permeation tests.

Diameter discs (16 mm) cut from the composite nanofiber membranes or casting films were placed on the mucosal surface. Samples (1 ml) were withdrawn from the receptor compartment at timed intervals, filtered through a 0.22 μm membrane (Millorpore, USA) and absorption was measured at 322 nm as before. All the measurements were carried out in triplicate.

3. Results and discussion

3.1. Morphology

Fig. 1(a) and (b) shows FESEM images of the composite nanofiber mat surface at different magnifications. The nanofibers have uniform structures without beads-on-a-string morphology, they had smooth surfaces and the matrix was free of any separating particles. The diameters of nanofibers were evenly distributed with an average of 254 ± 32 nm (Fig. 1c).

Fig. 1(d) shows FESEM images of the cross-section of the composite nanofibers. It is obvious that there are no any visible particles separating out from the nanofiber matrix, indicating that no phase separation had occurred during electrospinning. This also suggests that the molecules of the functional materials are uniformly distributed throughout the polymer matrix and so the system may be regarded as a solid solution.

FESEM images of the surface morphology (Fig. 1(e)) and cross-section (Fig. 1(f)) of the casting films, showed particles separating out and these could be seen both on the surface and in the cross-sections of the casting films, suggesting that the structures of casting films were not as homogeneous as those of electrospun fibers.

Electrospinning shares characteristics of both electrospraying and conventional solution dry spinning of fibers. Compared with the traditional SD evaporation methods, electrospun fibers are

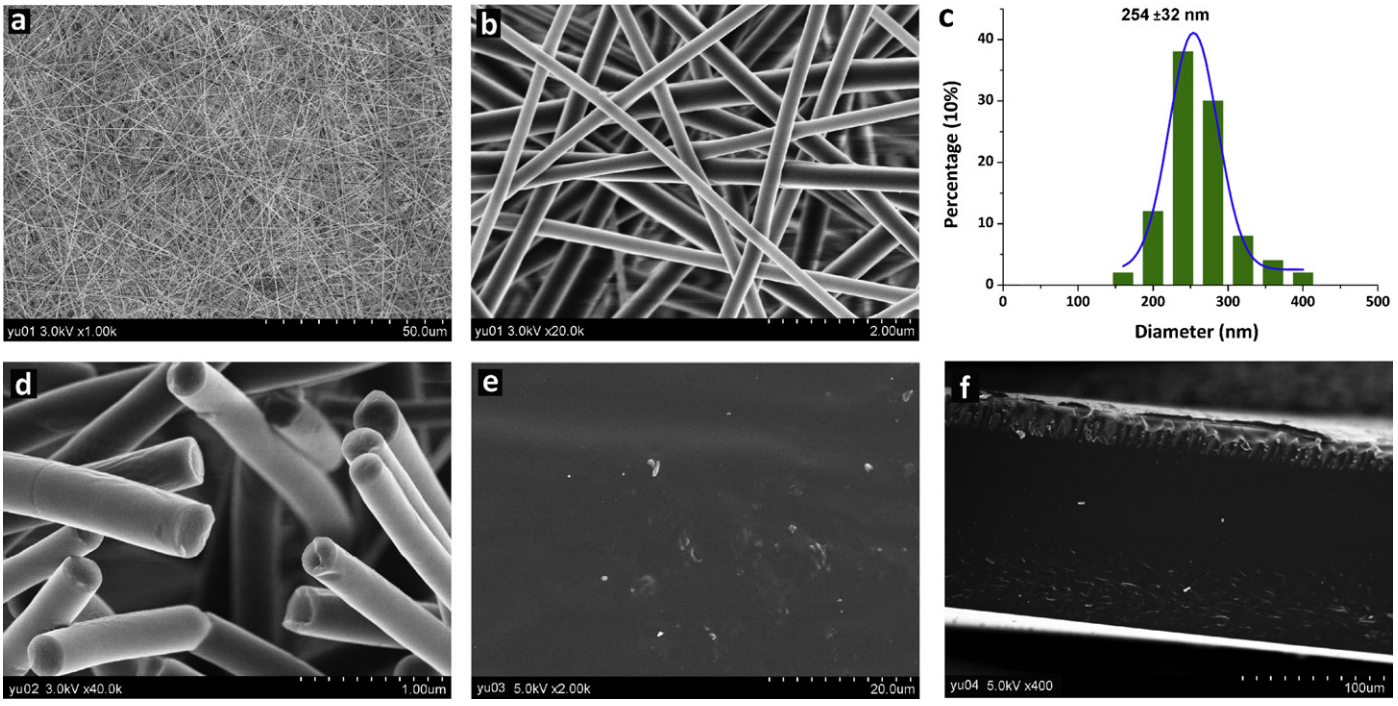

Fig. 1. FESEM images: (a) and (b) surface morphology of the composite nanofibers, (c) diameter distributions of the composite nanofibers, (d) cross-section of the composite nanofibers, (e) surface morphology of casting films and (f) cross-section of casting films.

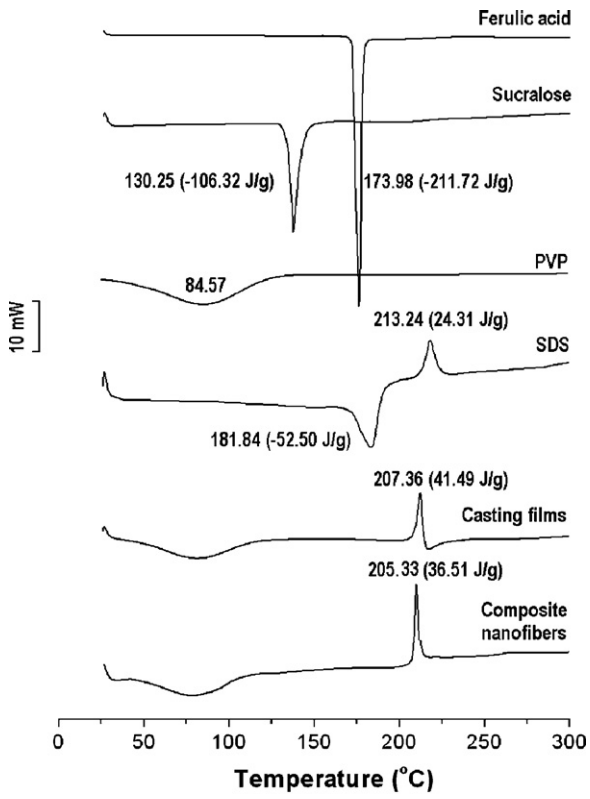

Fig. 2. DSC thermograms.

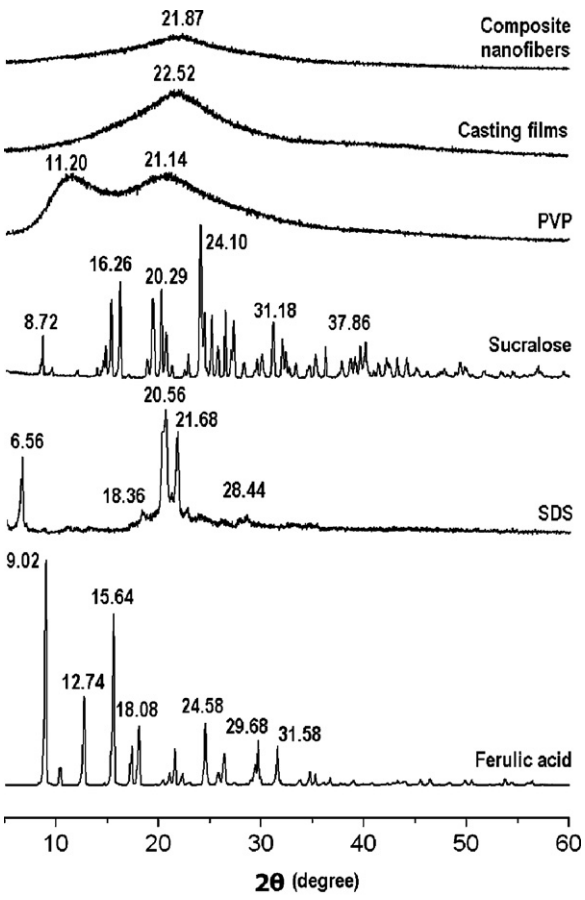

Fig. 3. X-ray diffraction patterns.

drawn from co-dissolving solutions within one second, avoiding the re-crystallization of drug during removal of the solvents, which is often a concern in traditional SDs preparation processes.

3.2. Physical status of the components in the electrospun fibers

DSC and XRD tests were undertaken to determine the physical status of the contained components in the composite nanofibers. The DSC thermograms are shown (Fig. 2) and the DSC curve of pure FA and sucralose exhibited a single endothermic response corresponding to melting points of 173.98 and 130.25 °C, respectively. SDS had a melting point of 181.84 °C followed by a decomposing temperature of 213.24 °C. PVP K30 had a broad endotherm due to dehydration, which lies between 80 and 120 °C and with a peak at 84.57 °C. PVP is a polymer and can be present in a glassy or rubber state. The change from one state to the other can be detected as a glass transition around 160–180 °C depending on its molecular weight (Jadhav et al., 2009). This glass transition is not visible in Fig. 2 due to scale.

DSC thermograms of both composite nanofibers and casting films did not show any melting peaks of small molecules, suggesting that FA, SDS and sucralose were no longer present as a crystalline material but had been converted into an amorphous state. However the decomposition bands of SDS in the composite nanofibers and casting films were narrower and higher than that of pure SDS. The peak temperatures of decomposition shifted from 213.24 to 207.36 °C for the casting films, and to 205.33 °C for the composite nanofibers, reflecting that the onset of SDS decomposition in fibers and casting films is earlier than that of pure SDS. The amorphous state of SDS and highly even distributions of SDS in fibers and casting films should make SDS molecules respond to the heat more sensitively than pure SDS crystalline particles, and the fibers and casting films might have better thermal conductivity than pure SDS. The combined effects of them promoted the SDS in fibers and casting films to decompose earlier and quicker.

As shown (Fig. 3), the presence of numerous distinct peaks in the XRD patterns indicated that FA, sucralose and SDS were present as crystalline materials with characteristic diffraction peaks. The PVP diffraction exhibits a diffused background pattern with two diffraction halos indicating that the polymer is amorphous (Mauro Banchero et al., 2007).

In respect to the composite nanofibers and the casting films the characteristic peaks of FA, sucralose and SDS were absent and there was only a characteristic hump of the amorphous forms. This suggests that all the small molecules were no longer present as crystalline material, but were fully converted into an amorphous state. The shape and the position of the amorphous haloes of the composite nanofibers and casting films were different from the pure PVP. The amorphous halo at 11.20° was absent in the XRD patterns of the composite nanofibers and casting films thus reflecting a change of the orientation, conformation and organization of polymer chains in the amorphous phase so altering of the amorphous packing properties and density of the polymer chains (Murthy et al., 1993).

Similarly the results from DSC and XRD demonstrated that the small functional molecules (FA, sucralose and SDS) were highly distributed in the PVP nanofiber matrix and were present in a complex manner where the original structure of pure materials was lost. This observation concurred with the findings from FESEM. Although particles were separated from the casting films in the FESEM images, the DSC and XRD results showed that the components are also in the amorphous form. This may be explained in terms of the separated particles having the same components but different compositions within the bulk films, or that the re-

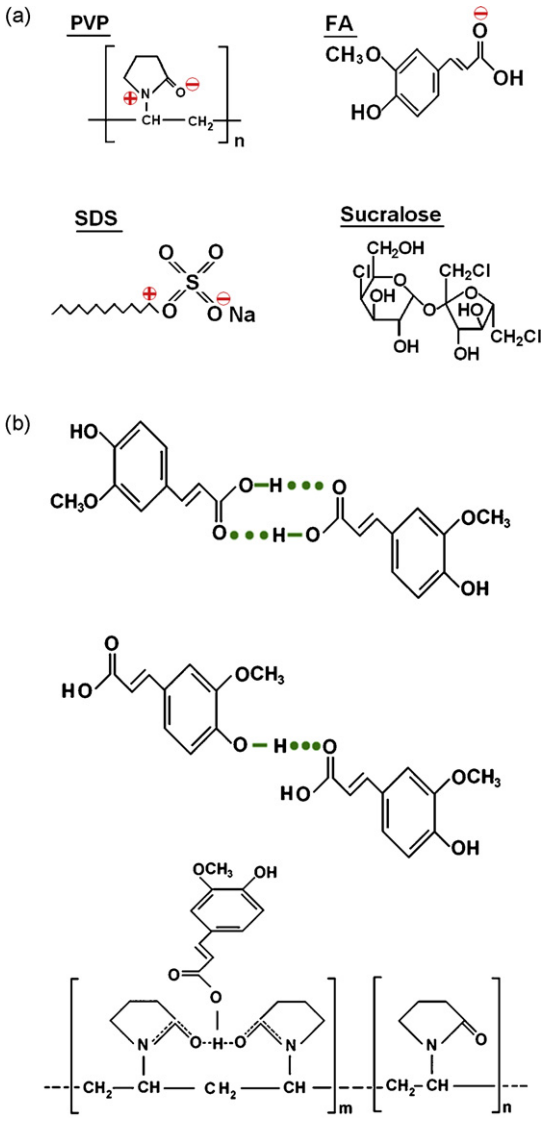

Fig. 4. Molecular structures of the components (a) and the hydrogen bonding between FA molecules and between FA and PVP molecules (b).

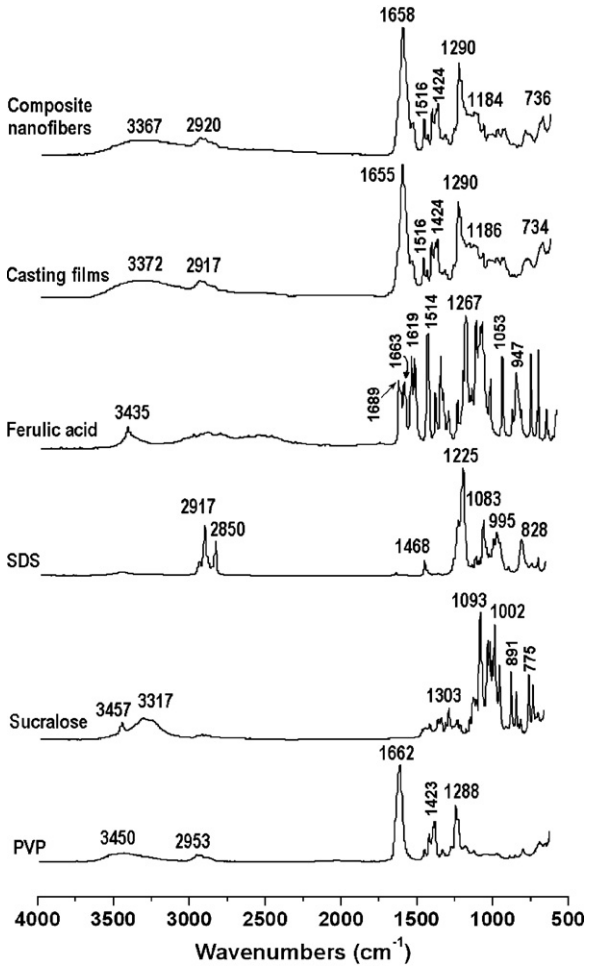

Fig. 5. ATR-FTIR spectra.

crystallized lattices were too small to be detected out under the conditions adopted.

3.3. The secondary-interactions among the components

The compatibility among the components is essential for producing high quality and the stability of the nanofibers. Often the second-order interactions such as hydrogen bonding, electrostatic interactions, and hydrophobic interactions would improve their compatibility (Yu et al., 2010c). The molecular structures of the four components are shown (Fig. 4a). FA and sucralose molecules possessed free hydroxyl groups and these could act as potential proton donors for hydrogen bonding. SDS molecules has S=O groups and PVP molecules has carbonyl groups and so could act as proton receptors. Therefore it can be speculated that the hydrogen bonding interactions can occur within the composite nanofibers through interactions with these groups.

FA molecules have both –OH groups and –C=O groups and in the FA crude particles a different type of hydrogen bonding between FA molecules is possible (Fig. 4b). This can be as verified by the ATR-FTIR spectra in which sharp peaks were visible for pure crystalline FA at 1689, 1663 and 1619 cm^{-1} (Fig. 5), representing the stretching vibration of –C=O groups in the different crystal lattice. However, all the peaks for FA disappeared in the composite nanofibers and casting films when samples were run in the ATR-FTIR spectra. Only one large peak at 1658 cm^{-1} for composite nanofibers, and at 1655 cm^{-1} for casting films was noted. This result indicates that there are fewer interactions between the FA molecules, but numerous hydrogen bonding formation between the PVP carbonyl group and the oxydryl group of the FA molecule (Fig. 4b). In relation to FA by interacting with the polymer the structure is less likely to form dimers that are necessary for the constructing the crystal lattice. The disappearance of multiple absorbance of –C=O groups in FA, the shift to a lower wave numbers of peaks assigned to the C=O stretching vibrations in PVP (from 1662 to 1658 cm^{-1} for composite nanofibers, and to 1655 cm^{-1} for the casting films), and the disappearance of multiple peaks within the 3000–4000 cm^{-1} regions (related to the O–H stretching vibrations in sucralose and FA) jointly demonstrated that hydrogen bonding was occurring.

The absorption bands of SDS (C–H stretching) at 2956, 2917 and 2850 cm^{-1} and of PVP (C–H stretching) at 2953 cm^{-1} were not present in the composite nanofibers when compared with single SDS and PVP. However a broader and weaker band at 2920 cm^{-1} appeared which is indicative of hydrophobic interactions between the PVP and SDS molecules. Although the electrostatic interactions cannot be determined from the ATR-FTIR spectra, they do exist between the negatively charged SDS head group and the nitrogen atom on the pyrrolidone ring of PVP (Pongpeerapat et al., 2006; Li et al., 1998) and also between the negatively charged PVP oxygen

(N^+ = C–O–) and the electron poor C-1′ of SDS (Roscigno et al., 2003; Ghebremeskel et al., 2007), as shown in Fig. 4a.

Based on the evidence presented here it is postulated that a combination of hydrogen bonding and some hydrophobic and electrostatic forces that provides an environment that stabilizes the structure so giving a high degree of compatibility between the components that make up the nanofibers. This in turn creates a homogeneous structure which influences both the stability of the SDs and the even dispersion of the drug so facilitating the dissolution of FA from the nanofibers.

3.4. Solubility and in vitro dissolution properties

FA has a UV absorbance peak at 322 nm, whereas the other components PVP, SDS and sucralose have no absorbance above 240 nm. Using this parameter the content of FA was determined by UV spectroscopy and samples were calculated from a calibration curve $A = 0.05774C - 0.00235$ ($R = 0.9996$) where C is the concentration of FA ($\mu g\,ml^{-1}$) and A is absorbance at 322 nm (linear range: 2–20 $\mu g\,ml^{-1}$).

FA as crude particles, in casting films and electrospun fibers at 37 °C had a solubility of 0.54 ± 0.05, 3.31 ± 0.17 and 3.27 ± 0.22 mg ml^{-1}, respectively. The presence of PVP and SDS in the aqueous solutions significantly improved the solubility of FA, which should be attributed to their good compatibility resulted from the secondary-interactions among them.

A comparison of *in vitro* dissolution profiles of FA from composite nanofibers, casting films, and crude FA particles ($\leq$100 μm) is shown in Fig. 6. The nanofiber mats and the casting films released 97.2% and 71.3% of the contained FA in the first minute respectively, and both exhausted all the FA after 10 min. Nevertheless when compared to the pure FA particles, which gave only 1.2% in the dissolution media in the first minute, it is clear that the third generation SDs presents a much faster dissolution.

The electrospun composite nanofibers have essential properties for improving the dissolution rates of poorly water-soluble drugs. (1) The composite nanofibers has a small diameter and a high surface to volume ratio, which means that there is a large surface area for the drug to be in contact with the dissolution media; (2) the nanofiber assembly has a three-dimensional continuous web structure which provides great porosity to facilitate the fast mass transformation of solvent and drug molecules from or to the bulk dissolution media; (3) a combination of the nanoscale diameters of the fibers which greatly decreases the diffusion layer thickness with the uniform PVP–SDS–FA–sucralose complex can improve the drug wettability; (4) the fast dissolution of the composite nanofibers could augment the local concentrations of supersaturated drug solution, especially in the presence of PVP and SDS and thus correspondingly increase the drug gradients for rapid diffusion of molecules to the dissolution media. The combined synergistic effect of nanosizing of fibers, continuous web structure of the composite nanofibers and molecular distributions of drug in the filament-forming matrix provide the composite nanofibers with unique properties for improving the dissolution rate of FA.

In comparison the casting films had a compact structure which has a limited surface area and so has matrix that lacks porosity for quick transfer of solvent and drug molecules. The casting films dissolved gradually through a 'polymer-controlled' mechanism (Rangel-Yagui et al., 2005; Ghebremeskel et al., 2007; Doherty and York, 1987) by the erosion of the surface film as one layer followed another throughout the process, which delayed the dissolution of the contained FA to some extent. Nevertheless the key factor that played a decisive role was the amorphous state of FA in the third generation SDs, by which the casting films also presented a much faster dissolution rate than pure FA.

3.5. In vitro permeation properties

The buccal mucosae were used to conduct the *in vitro* permeation study here because the electrospun fiber mats have the potentional to develop oral fast-dissolving drug delivery membrane. Discs cut from the nanofiber mats and casting films for *in vitro* permeation were compared. The casting films had an average thickness of 0.157 ± 0.02 mm and a weight of 32.34 ± 0.34 mg ($n = 6$), giving an apparent density of 1.02 mg cm^{-3}. The electrospinning composite nanofibers had a thickness of 0.78 ± 0.06 mm and a weight of 33.51 ± 0.46 mg. The apparent densities of the electrospun membrane were 0.21 mg cm^{-3}. 10 mg of the crude FA particles were spread on the mucosal surface evenly as control.

Comparison of *in vitro* permeation profiles of FA from composite nanofibers, casting films, and crude FA particles is shown in Fig. 7. The cumulative permeation percentage after 1 h for the composite nanofibers, casting films, and crude FA particles were 50.3%, 18.4% and 5.83%, respectively. Regression values from the linear release time equations were estimated for the composite nanofibers, casting films, and crude FA particles and these were $Q = 0.0531t + 0.5592$ ($R = 0.9637$, $t \leq 120$ min), $Q = 0.0237t + 0.3322$ ($R = 0.9900$, $t \leq 240$ min), $Q = 0.0041t + 0.0265$ ($R = 0.9992$, $t \leq 300$ min), respectively, where Q is the proportion of FA permeated and t is the time in min. Thus the composite nanofibers, casting films, and crude FA particles had a permeation rate of 20.42, 9.12, and 1.57 $\mu g\,min^{-1}\,cm^{-2}$, respectively.

The composite nanofibers yielded a permeation rate of FA that was over 13-fold faster than that of the crude particles, and dou-

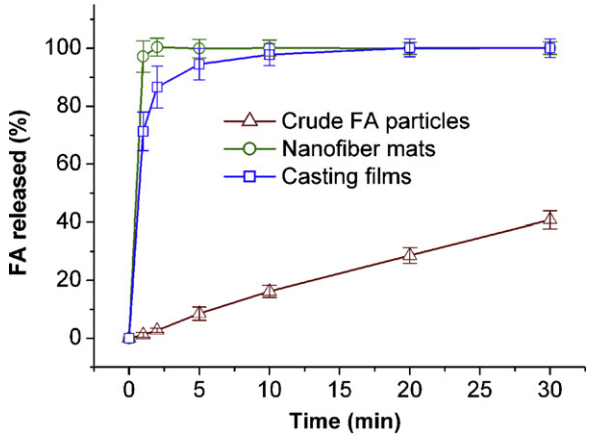

Fig. 6. *In vitro* dissolution profiles ($n = 3$).

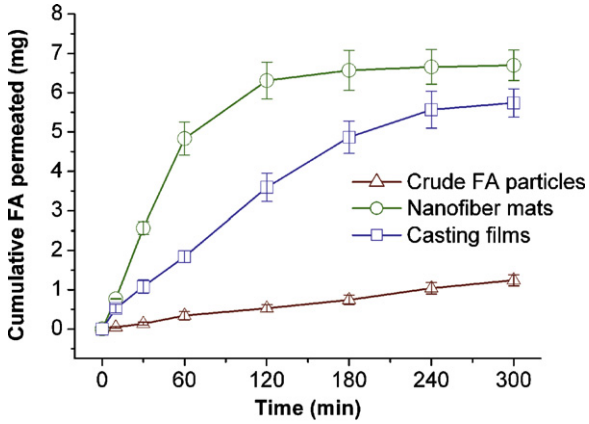

Fig. 7. *In vitro* permeation profiles ($n = 3$).

ble fold faster than the casting films. The faster permeation rates from the composite nanofibers can be explained in terms that: the permeability across the sublingual mucosa is a passive diffusion process and hence faster dissolution of FA would lead to an increased concentration gradient of drug at the mucosal surface. This would facilitate rapid partitioning of drug into the sublingual mucosae and subsequent permeation (Chett et al., 2001). The SDS released from the nanofibers may also improve permeation by extracting intercellular lipids that act as a rate-limiting barrier to the transport of FA molecules (Nicolazzo et al., 2005).

In addition to the advantages of improving solubility behavior and permeation properties of FA, the third SDs are easier to be post-processed as they have good drug stability because of the steric constraint provided by the small diameter of nanofibers. This avoids the re-crystallization and possible growth of the crystal lattice.

Within this context the artificial sweetener, sucralose has gained popularity recently because it is 600 times more effective by weight compared to sucrose and does not have the bitter aftertaste attributed to many non-nutritive sweeteners. Sucralose, FDA approved is now applied as a general-purpose sweetener in foods, beverages, dietary supplements and medical foods (Mead et al., 2009; Grotz and Munro, 2009).

4. Conclusions

Third generation SDs of FA in composite nanofibers with three-dimensional continuous web structure has been successfully prepared using electrospinning process from co-dissolving solutions of FA, PVP, SDS and sucralose. The nanofibers had smooth surface with an average diameter of 254 ± 32 nm. DSC and XRD results demonstrated that FA, SDS, and sucralose were well distributed in the PVP fiber matrix in an amorphous state due to the second-order interactions. *In vitro* dissolution and permeation tests showed that the nanofiber-based SDs could rapidly release all the FA within in 1 min and had a 13-fold greater permeation rate across sublingual mucosa compared to crude FA particles. The casting films have the same compositions as the composite nanofibers and belong to the third generation SDs, they gave the same solubility of FA as the composite nanofibers, and also exhibited a much faster dissolution rate than pure FA particles. In conclusion we believe we have developed an electrospinning system that can be used in the construction of polymers containing functional materials under conditions that control the chemical compositions of the nanofibers. This study also provides future strategies for developing third generation SDs with structural characteristics for enhancing absorbance and delivery of poorly water-soluble drugs.

Acknowledgements

This work was financially supported by China Postdoctoral Science Foundation (Special Grade No. 200902195) and UK–CHINA Joint Laboratory for Therapeutic Textiles, and the Fundamental Research Funds for the Central Universities in China (No. 2010C03-2-1).

References

Anselmi, C., Centini, M., Maggiore, M., Gaggelli, N., Andreassi, M., Buonocore, A., Beretta, G., Facino, R.M., 2008. Non-covalent inclusion of ferulic acid with α-cyclodextrin improves photo-stability and delivery: NMR and modeling studies. J. Pharm. Biomed. Anal. 46, 645–652.

Burke, M.D., Luzhansky, D., 2007. Nanofiber-based drug delivery. In: Thassu, D. (Ed.), Nanoparticulate Drug Delivery Systems. Informa Healthcare, ISBN 978-0-8493-9073-9, pp. 61–62 (Chapter 4).

Chett, D.J., Chen, L.H., Chien, Y.W., 2001. Characterization of captopril sublingual permeation of preferred routes and mechanisms. J. Pharm. Sci. 90, 1868–1877.

Chokshi, R.J., Zia, H., Sandhu, H.K., Shah, N.H., Malick, W.A., 2007. Improving the dissolution rate of poorly water-soluble drug by solid dispersion and solid solution – pros and cons. Drug Deliv. 14, 33–45.

Dhirendra, K., Lewis, S., Udupa, N., Atin, K., 2009. Solid dispersions: a review. Pak. J. Pharm. Sci. 22, 234–246.

Doherty, C., York, P., 1987. Mechanism of dissolution of frusemide/PVP solid dispersions. Int. J. Pharm. 34, 197–205.

Doshi, J., Reneker, D.H., 1995. Electrospinning process and applications of electrospun fibers. Electrostatics 35, 151–160.

Dzenis, Y., 2004. Spinning continuous fibres for nanotechnology. Science 304, 1917–1919.

Formhals, A. 1934. Process and apparatus for preparing artificial threads. US Patent 1975504, October 2.

Ghebremeskel, A.N., Vemavarapu, C., Lodaya, M., 2007. Use of surfactants as plasticizers in preparing solid dispersions of poorly soluble API: selection of polymer–surfactant combinations using solubility parameters and testing the processability. Int. J. Pharm. 328, 119–129.

Grotz, V.L., Munro, I.C., 2009. An overview of the safety of sucralose regulatory. Toxicol. Pharmacol. 55, 1–5.

Huang, Z.M., Zhang, Y.Z., Kotaki, M., Ramakrishna, S., 2003. A review on polymer nanofibers by electrospinning applications in nanocomposites. Compos. Sci. Technol. 63, 2223–2253.

Jadhav, N.R., Gaikwad, V.L., Nair, K.J., Kadam, H.M., 2009. Glass transition temperature: basics and application in pharmaceutical sector. Asian J. Pharm. 3, 82–89.

Kampa, M., Alexaki, V.I., Notas, G., Nifli, A.P., Nistikaki, A., Hatzoglou, A., Bakogeorgou, E., Kouimtzoglou, E., Blekas, G., Boskou, D., Gravanis, A., Castanas, E., 2004. Antiproliferative and apoptotic effects of selective phenolic acids on T47D human breast cancer cells: potential mechanisms of action. Breast Cancer Res. 6, 63–74.

Lee, Y.S., 2005. Role of NADPH oxidase-mediated generation of reactive oxygen species in the mechanism of apoptosis induced by phenolic acids in HepG2 human hepatoma cells. Arch. Pharm. Res. 28, 1183–1189.

Leuner, C., Dressman, J., 2000. Improving drug solubility for oral delivery using solid dispersions. Eur. J. Pharm. Biopharm. 50, 47–60.

Li, D., Xia, Y.N., 2004. Electrospinning of nanofibers: reinventing the wheel. Adv. Mater. 16, 1151–1170.

Li, F., Li, G.Z., Xu, G.Y., Wang, H.Q., Wang, M., 1998. Studies on the interactions between anionic surfactants and polyvinylpyrrolidone: surface tension measurement, ^{13}C NMR and ESR. Colloid Polym. Sci. 276, 1–10.

Mauro Banchero, L.M., Ada Ferri, D.S., Ronchetti, S., Sicardi, S., 2007. Impregnation of PVP microparticles with ketoprofen in the presence of supercritical CO_2. J. Supercrit. Fluids 42, 378–384.

Mead, R.N., Morgan, J.B., Avery Jr., G.B., Kieber, R.J., Kirk, A.M., Skrabal, S.A., Willey, J.D., 2009. Occurrence of the artificial sweetener sucralose in coastal and marine waters of the United States. Mar. Chem. 116, 13–17.

Murthy, N.S., Minor, H., Bednarczyk, C., Krimm, S., 1993. Structure of the amorphous phase in oriented polymers. Macromolecules 26, 1712–1721.

Nicolazzo, J.A., Reed, B.L., Finnin, B.C., 2005. Buccal penetration enhancers – how do they really work? J. Control. Release 105, 1–15.

Pongpeerapat, A., Higashi, K., Tozuka, Y., Moribe, K., Yamamoto, K., 2006. Molecular interaction among probucol/PVP/SDS multicomponent system investigated by solid-state NMR. Pharm. Res. 23, 2566–2574.

Rangel-Yagui, C.O., Junior, A.P., Tavares, L.C., 2005. Micellar solubilization of drugs. J. Pharm. Pharm. Sci. 8, 147–165.

Roscigno, P., Asaro, F., Pellizer, G., Ortana, O., Paduano, L., 2003. Complex formation between PVP and sodium decyl sulfate. Langmuir 19, 9638–9644.

Sohn, Y.T., Oh, J.H., 2003. Characterization of physicochemical properties of ferulic acid. Arch. Pharm. Res. 26, 1002–1008.

Yu, D.G., Shen, X.X., Branford-White, C., White, K., Zhu, L.M., Bligh, S.W.A., 2009a. Oral fast-dissolving drug delivery membranes prepared from electrospun PVP ultrafine fibers. Nanotechnology 20, 055104.

Yu, D.G., Zhu, L.M., White, K., Branford-White, C., 2009b. Electrospun nanofiber-based drug delivery systems. Health I, 67–75.

Yu, D.G., Branford-White, C., Shen, X.X., Zhang, X.F., Zhu, L.M., 2010a. Solid dispersions of ketoprofen in drug-loaded electrospun nanofibers. J. Disper. Sci. Technol. 31, 902–908.

Yu, D.G., Branford-White, C., White, K., Li, X.L., Zhu, L.M., 2010b. Comparison of solid dispersions in drug delivery membranes from different processes. AAPS PharmSciTech 11, 809–817.

Yu, D.G., Branford-White, C., Li, L., Wu, X.M., Zhu, L.M., 2010c. The compatibility of acyclovir with the matrix polymer PAN in the electrospun nanofiber membrane. J. Appl. Polym. Sci. 117, 1509–1515.

Vasconcelos, T., Sarmento, B., Costa, P., 2007. Solid dispersions as strategy to improve oral bioavailability of poor water soluble drugs. Drug Discov. Today 12, 1068–1075.

Verreck, G., Chun, I., Peeters, J., Rosenblatt, J., Brewster, M.E., 2003. Preparation and characterization of nanofibers containing amorphous drug dispersion generated by electrostatic spinning. Pharm. Res. 20, 810–817.